

I. INTRODUCTION

A. Motivation

For many standard channel models, such as additive Gaussian noise and fading channels with receive Channel State Information (CSI), the design of optimal demodulators and decoders is well-understood. Most communication links hence use pilot sequences to estimate CSI, which is then plugged into the optimal receiver with ideal receive CSI (see, e.g., [1]). This standard model-based approach is inapplicable if: (i) an accurate channel model is unavailable; and/or (ii) the optimal receiver for the given transmission scheme and channel is of prohibitive complexity or unknown. Examples of both scenarios are reviewed in [3], [4], and include new communication set-ups, such as molecular channels, which lack well-established models; and links with strong non-linearities, such as satellite links with non-linear transceivers, whose optimal demodulators can be highly complex [3], [5]. This observation has motivated a long line of work on the application of machine learning methods to the design of demodulators or decoders, from the 90s [3] to many recent contributions, including [6], [7], [8] and references therein.

Demodulation and decoding can be interpreted as classification tasks, whereby the input is given by the received baseband signals and the output consists of the transmitted symbols, for demodulation, and of the transmitted binary messages, for decoding. Pilot symbols can hence be used as training data to carry out the supervised learning of a parametric model for the demodulator or decoder, such as Support Vector Machines (SVMs) or neural networks. The performance of the trained “machine” as a demodulator or a decoder generally depends on how representative the training data is for the channel conditions encountered during test time and on the suitability of the parametric model in terms of trade-off between bias and variance.

To the best of our knowledge, all the prior works reviewed above assume that training is carried out using pilot signals from the same transmitter whose data is to be demodulated or decoded. This generally requires the transmission of long pilot sequences for training. In this paper, we consider an Internet-of-Things (IoT)-like scenario, illustrated in Fig. 1, in which devices transmit sporadically using short packets with few pilot symbols. The number of pilots is generally insufficient to obtain an accurate estimate of the end-to-end channel, which generally includes the effects of fading and of the transmitter’s non-linearities [9]. We propose to tackle this problem by using *meta-learning* [10].

B. Meta-Learning

Meta-learning, also sometimes referred to as “learning to learn”, aims at leveraging training and test data from different, but related, tasks for the purpose of acquiring an inductive bias that is suitable for the entire class of tasks of interest [10]. The inductive bias can take different forms, such as a learning

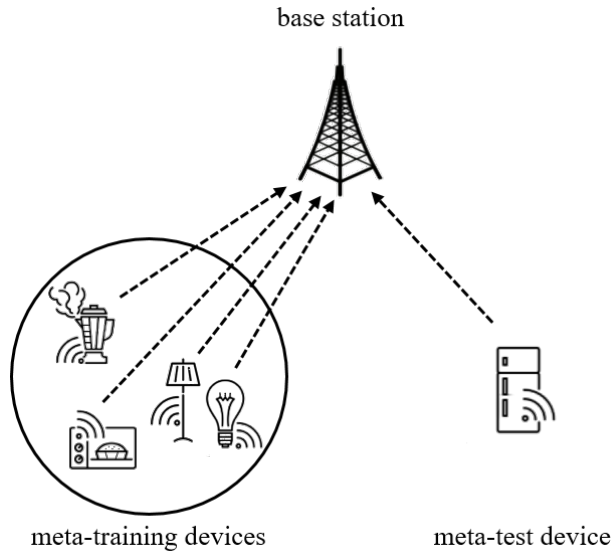


Fig. 1. Illustration of few-pilot training for an IoT system via meta-learning.

procedure, an initialization of model parameters, or a prior over the model parameters [11]. An important application of meta-learning is the acquisition of a learning algorithm, or of a model prior, that allow a quick adaptation to a new, but related, task using few training examples, also known as *few-shot learning* [12]. For instance, one may have training and test labelled images for binary classifiers of different types of objects, such as cats vs dogs or birds vs bikes, which can be used as meta-training data to quickly learn a new binary classifier, say for handwritten digits, from a few training examples.

Meta-learning has recently received renewed attention, particularly thanks to advances in the development of methods based on Stochastic Gradient Descent (SGD), including Model-Agnostic Meta-Learning (MAML) [13], REPTILE [14], and fast Context Adaptation VIA meta-learning (CAVIA) [15]. Such techniques can be generally classified as either *offline*, whereby the meta-training data is fixed and given [13], [14], [15]; or *online*, whereby all prior data from related tasks is treated as meta-training data in a streaming fashion [16].

C. Main Contributions

As illustrated in Fig. 2 and Fig. 3, the key idea of this paper is to use pilots from previous transmissions of other IoT devices as meta-training data in order to train a procedure that is able to quickly adapt a demodulator to new end-to-end channel conditions from few pilots. We consider both an offline formulation, whereby the set of previous transmissions is fixed, and an online set-up, in which the meta-training set is updated as transmitted pilots are received. The main contributions are as follows:

- We adapt to the problem at hand a number of state-of-the-art offline meta-learning solutions, namely

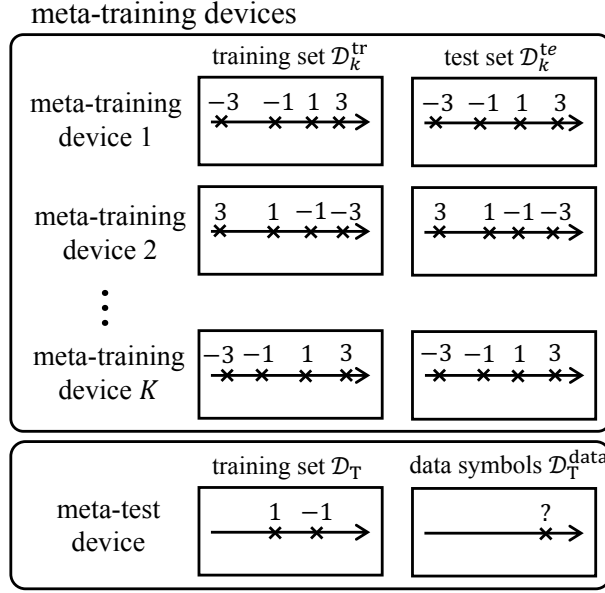


Fig. 2. Offline meta-learning: Meta-training and meta-test data for 4-PAM transmission from set $\mathcal{S} = \{-3, -1, 1, 3\}$. The figure assumes $N = 8$ pilot symbols divided into $N^{\text{tr}} = 4$ for meta-training and $N^{\text{te}} = 4$ for meta-testing, and $P = 2$ pilots for the meta-test device. Crosses represent received signals $y_k^{(n)}$, and the number above each cross represents the corresponding label, i.e., the pilot symbol $s_k^{(n)}$.

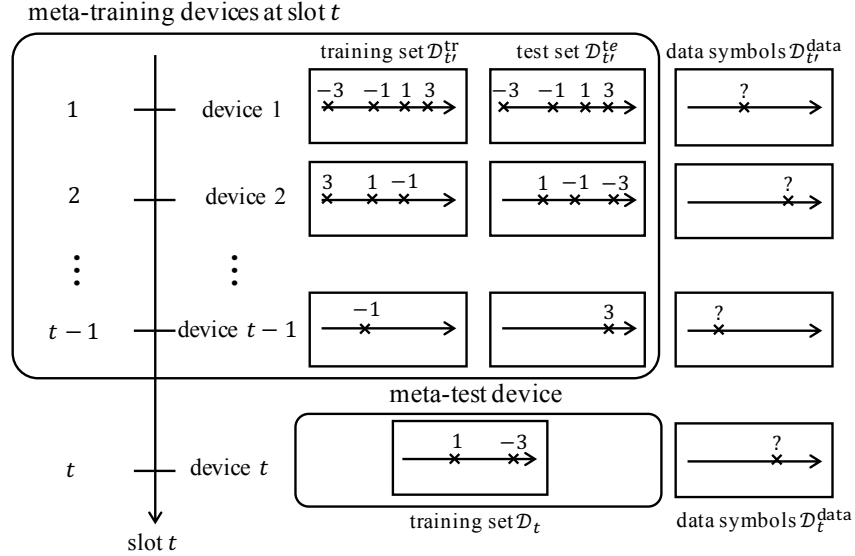


Fig. 3. Online meta-learning: Meta-training and meta-test data for 4-PAM transmission from set $\mathcal{S} = \{-3, -1, 1, 3\}$. Meta-training data are accumulated as the BS observes subsequent slots $t = 1, 2, \dots$, with one device transmitting pilots and data symbols in each slot.

MAML [13], FOMAML [13], REPTILE [14], and CAVIA [15]. We discuss their relative merits and provide a unified interpretation in terms of the Expectation-Maximization (EM) algorithm;

- We validate the advantage of meta-learning with extensive numerical results, and provide a comparative study of the performance of various meta-learning solutions;
- We propose a novel online solution that integrates meta-learning with an adaptive selection of the

number of pilots. We compare the proposed solution with conventional non-adaptive solutions in terms of receiver's performance and number of pilots.

The results in this paper have been partially presented in [2]. In particular, reference [2] derives an offline MAML-based algorithm, and offers some preliminary numerical results. To the best of our knowledge, the only other prior works that apply meta-learning to communication problems are [17] and [18]. In [17], which is concurrent to [2], the authors train a neural network-based decoder that can adapt to the new channel condition with a minimal number of pilot symbols using meta-learning via FOMAML. In [18], the authors train a neural network-based channel estimator in OFDM system with meta-learning via FOMAML in order to obtain an effective channel estimation given a small number of pilots.

The rest of the paper is organized as follows. In Sec. II we detail system model and offline meta-learning problem. In Sec. III we organize various meta-learning solutions with an unified interpretation. In Sec. IV we redefine system model for an online setting and propose a novel online solution, including adaptive pilot allocation. Numerical results are presented in Sec. V and conclusions and extensions are proposed in Sec. VI.

II. MODEL AND PROBLEM

A. System Model

In this paper, we consider the IoT system illustrated in Fig. 1, which consists of a number of devices and a base station (BS). For each device k , we denote by $s_k \in \mathcal{S}$ and y_k the complex symbol transmitted by the device and the corresponding received signal at the BS, respectively. We also denote by \mathcal{S} the set of all constellation symbols as determined by the modulation scheme. The end-to-end channel for a device k is defined as

$$y_k = h_k x_k + z_k, \quad (1)$$

where h_k is the complex channel gain from device k to the BS, which we assume to be constant over the transmission of interest; $z_k \sim \mathcal{CN}(0, N_0)$ is additive white complex Gaussian noise; and

$$x_k \sim p_k(\cdot | s_k) \quad (2)$$

is the output of a generally random transformation defined by the conditional distribution $p_k(\cdot | s_k)$. This conditional distribution accounts for transmitter's non-idealities such as phase noise [19], I/Q imbalance [20], and amplifier's characteristics [9] of the IoT device. As an example, a common model that assumes only amplitude distortion is defined by the non-linear deterministic mapping [5]

$$x_k = \frac{\alpha_k |s_k|}{1 + \beta_k |s_k|^2} \exp(j \angle s_k), \quad (3)$$

where $\angle s_k$ represents the phase of symbol s_k , and α_k and β_k are constants depending on the characteristics of the device.

Based on the reception of a few pilots from a target device, we aim at determining a demodulator that recovers the transmitted symbol s from the received signal y with high probability. The demodulator is defined by a conditional probability distribution $p(s|y, \varphi)$, which depends on a trainable parameter vector φ .

B. Offline Meta-Learning Problem

Following the nomenclature of meta-learning [13], we refer to the target device as the *meta-test device*. To enable few-pilot learning, we assume here that the BS can use the signals received from the previous pilot transmissions of K other IoT devices, which are referred to as *meta-training devices* and their data as *meta-training data*. Specifically, as illustrated in Fig. 2, the BS has available N pairs of pilot s_k and received signal y_k for each meta-training device $k = 1, \dots, K$. The meta-training dataset is denoted as $\mathcal{D} = \{\mathcal{D}_k\}_{k=1, \dots, K}$, where $\mathcal{D}_k = \{(s_k^{(n)}, y_k^{(n)}) : n = 1, \dots, N\}$, and $(s_k^{(n)}, y_k^{(n)})$ are the pilot-received signal pairs for the k th meta-training device. This scenario is referred to as offline meta-learning since the meta-training dataset \mathcal{D} is fixed and given. Online meta-training will be discussed in Sec. IV.

For the target, or the meta-test, device, the BS receives P pilot symbols. We collect the P pilots received from the target device in set $\mathcal{D}_T = \{(s^{(n)}, y^{(n)}) : n = 1, \dots, P\}$. The demodulator can be trained using meta-training data \mathcal{D} and the pilot symbols \mathcal{D}_T from the meta-test device.

Training requires the selection of a parametric model $p(s|y, \varphi)$ for the demodulator. The choice of the parametric model $p(s|y, \varphi)$ should account for the standard trade-off between capacity of the model and overfitting [21], [22]. To fix the ideas, we will assume that the demodulator $p(s|y, \varphi)$ is given by a multi-layer neural network with L layers, with a softmax non-linearity in the final, L th, layer. This can be written as

$$p(s|y, \varphi) = \frac{\exp\left([f_{\varphi^{(L-1)}}(f_{\varphi^{(L-2)}}(\cdot \cdot f_{\varphi^{(1)}}(y)))\right]_s}{\sum_{s' \in \mathcal{S}} \exp\left([f_{\varphi^{(L-1)}}(f_{\varphi^{(L-2)}}(\cdot \cdot f_{\varphi^{(1)}}(y)))\right]_{s'}}, \quad (4)$$

where $f_{\varphi^{(l)}}(x) = \sigma(W^{(l)}x + b^{(l)})$ represents the non-linear activation function of the l th layer with parameter $\varphi^{(l)} = \{W^{(l)}, b^{(l)}\}$, with $W^{(l)}$ and $b^{(l)}$ being the weight matrix and bias vector of appropriate size, respectively; $[\cdot]_s$ stands for the element regarding s ; and $\varphi = \{\varphi^{(l)}\}_{l=1, \dots, L-1}$ is the vector of parameters. The non-linear function $\sigma(\cdot)$ can be, e.g., a ReLU or a hyperbolic tangent function. The input y in (1) can be represented as a two-dimensional vector comprising real and imaginary parts of the received signal.

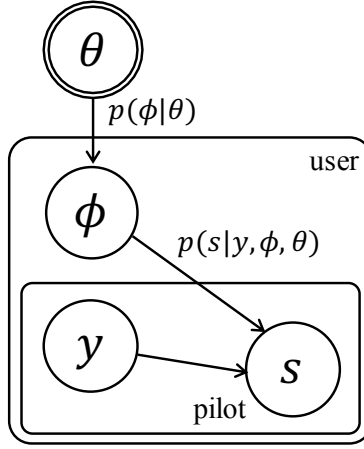


Fig. 4. Graphical model assumed by meta-learning: The demodulator $p(s|y, \phi, \theta)$ depends on a user-specific, or context, random variable ϕ , as well as on a shared parameter θ , which may also affect the prior distribution of the context variable ϕ . Double circles denote parameters, and the tile notation (see, e.g., [24]) defines multiple users and pilots per user.

III. OFFLINE META-LEARNING ALGORITHMS

In this section, we adapt state-of-the-art offline meta-learning algorithms for the design of demodulator (4) given meta-training and meta-test data. As discussed in Sec. I, we view demodulation as a classification task. To set the notation, for any set \mathcal{D}_0 of pairs (s, y) of transmitted symbol s and received signal y , we define the standard cross-entropy loss function as a function of the demodulator parameter vector φ as

$$L_{\mathcal{D}_0}(\varphi) = - \sum_{(s,y) \in \mathcal{D}_0} \log p(s|y, \varphi). \quad (5)$$

A. Joint Training

As a benchmark, we start by considering a conventional approach that uses the meta-training data \mathcal{D} and the training data \mathcal{D}_T for the *joint training* of the model $p(s|y, \varphi)$. Joint training pools together all the pilots received from the meta-training devices and the meta-test device, and carries out the optimization of the cumulative loss $L_{\mathcal{D} \cup \mathcal{D}_T}(\varphi)$ in (5) using SGD. Accordingly, the parameter vector φ is updated iteratively based on the rule

$$\varphi \leftarrow \varphi + \eta \nabla_{\varphi} \log p(s^{(n)}|y^{(n)}, \varphi), \quad (6)$$

by drawing one pair $(s^{(n)}, y^{(n)})$ at random from the set $\mathcal{D} \cup \mathcal{D}_T$. In (6), the step size η is assumed to be fixed for simplicity of notation but it can in practice be adapted across the updates (see, e.g., [23]). Furthermore, this rule can be generalized by summing the gradient in (6) over a minibatch of pairs from the dataset $\mathcal{D} \cup \mathcal{D}_T$ at each iteration [23].

B. A Unified View of Meta-Learning

A useful way to introduce meta-learning in terms of the graphical model is illustrated in Fig. 4. Accordingly, meta-learning assumes a demodulator $p(s|y, \phi, \theta)$ that depends on a shared parameter θ common to all tasks, or users, and on a latent context variable ϕ , which is specific to a user. The specific parameterization $p(s|y, \phi, \theta)$ and its relationship with (4) depend on the meta-learning scheme, and they will be discussed below. Note that, as illustrated in Fig. 4, the context vector ϕ is assumed to be random, while θ is a shared (deterministic) parameter. Furthermore, from Fig. 4, the shared variable θ can also affect the prior distribution of the context variable ϕ . In this framework, the key idea is that meta-training data \mathcal{D} is used to estimate the shared parameters θ via the process of meta-training, while the context variable ϕ is inferred from the meta-test data \mathcal{D}_T .

To elaborate, a principled way to train the model in Fig. 4 would be to estimate parameter θ using the Expectation-Maximization (EM) algorithm based on the meta-training data \mathcal{D} . The EM algorithm is in fact the standard tool to tackle the problem of maximum likelihood estimation in the presence of latent variables, here the context variables ϕ (see, e.g., [21], [22], [24]). EM maximizes the sum of marginal likelihoods

$$p(s|y, \theta) = \mathbb{E}_{\phi \sim p(\phi|\theta, \mathcal{D}_k)}[p(s|y, \phi, \theta)] \quad (7)$$

over the data pairs (s, y) from all data sets \mathcal{D}_k in the meta-training data set \mathcal{D} . In (7), the average is taken with respect to the posterior distribution $p(\phi|\theta, \mathcal{D}_k)$ of the context variable given the training data \mathcal{D}_k of the k th meta-training device. After EM training, one can consider the obtained parameter θ as fixed when inferring a data symbol s given a new observed signal y and the pilots \mathcal{D}_T for the meta-test device. This last step would ideally yield the demodulator

$$p(s|y, \theta) = \mathbb{E}_{\phi \sim p(\phi|\theta, \mathcal{D}_T)}[p(s|y, \phi, \theta)], \quad (8)$$

where the average is taken over the posterior distribution $p(\phi|\theta, \mathcal{D}_T)$ of the context variable given the training data of the meta-test device.

The computation of the posteriors $p(\phi|\theta, \mathcal{D}_k)$ in (7) and $p(\phi|\theta, \mathcal{D}_T)$ in (8) are generally of infeasible complexity. Therefore, state-of-the-art meta-learning techniques approximate this principled solution by either employing point estimate of latent context variable ϕ [13], [14], [15] or by direct estimation of its posterior distribution [25], [26], [27]. In this paper, we focus on the more common point estimate based meta-learning techniques, which are reviewed next.

C. MAML

For any meta-training device k , MAML [13] assumes a demodulator $p(s|y, \phi_k)$ given by (4) with model weights φ equal to the context variable ϕ_k . The user-specific variable ϕ_k , rather than being obtained from

the ideal posterior $p(\phi_k|\theta, \mathcal{D}_k)$ as in (7), is computed via SGD-based training from the data \mathcal{D}_k . Specifically, the key idea in MAML is to identify during meta-training an initial shared parameter θ such that, starting from it, the SGD updates (6) using pilots from \mathcal{D}_k produce a parameter vector ϕ_k that yields a low value of the loss function (5) for any meta-training device k (i.e., for $\mathcal{D}_0 = \mathcal{D}_k$). As we will detail, it is possible to consider one or multiple SGD updating steps (6) [28]. After meta-training, the initial parameter θ is used for the SGD updates of the target device based on the pilots in set \mathcal{D}_T .

To elaborate, assume first that we had available the exact average loss $L_k(\phi_k) = \mathbb{E}[-\log p(s_k|y, \phi_k)]$ for all meta-training devices $k = 1, \dots, K$. The average in $L_k(\phi_k)$ is taken over the distribution $p(s_k, y) = p(s_k)p(y|s_k)$, where $p(s_k)$ is the prior distribution of the transmitted symbol s_k and $p(y|s_k)$ is defined by (1). Note that in practice this information is not available since the channel and the transmitters' model are not known a priori. During meta-training, MAML seeks an initial value θ such that, for every device k , the losses $L_k(\phi_k)$ obtained after one or more SGD updates starting from θ are collectively minimized. As discussed, the SGD updates can be interpreted as producing a point estimate of the context variables ϕ_k in the model in Fig. 4 [11]. Mathematically, with a single SGD iteration, we obtain the estimate

$$\phi_k = \theta - \eta \nabla_{\theta} L_k(\theta). \quad (9)$$

More generally, with $m \geq 1$ local SGD updates we obtain $\phi_k = \phi_k^m$, where

$$\phi_k^i = \phi_k^{i-1} - \eta \nabla_{\phi_k^{i-1}} L_k(\phi_k^{i-1}), \quad (10)$$

for $i = 1, \dots, m$, with $\phi_k^0 = \theta$. The identification of a shared parameter θ is done by minimizing the sum $\sum_{k=1}^K L_k(\phi_k)$ over θ .

The losses $L_k(\phi_k)$ for all meta-training devices are not known and need to be estimated from the available data. To this end, in the meta-training phase, each set \mathcal{D}_k of N pairs of pilots and received signals for meta-training device k is randomly divided into a training set $\mathcal{D}_k^{\text{tr}}$ of N^{tr} pairs and a test set $\mathcal{D}_k^{\text{te}}$ of N^{te} pairs, as shown in Fig. 2. The updated context variable ϕ_k is computed by applying the SGD-based rule in (6) over all pairs in training subset $\mathcal{D}_k^{\text{tr}}$, as in (10), e.g., $\phi_k = \theta - \eta \nabla_{\theta} L_{\mathcal{D}_k^{\text{tr}}}(\theta)$ for a single update. The loss $L_k(\phi_k)$ is then estimated by using the test subset $\mathcal{D}_k^{\text{te}}$ as $L_{\mathcal{D}_k^{\text{te}}}(\phi_k)$. Finally, MAML minimizes the overall estimated loss $\sum_{k=1}^K L_{\mathcal{D}_k^{\text{te}}}(\phi_k)$ by performing an SGD-based update in the direction of the gradient $\nabla_{\theta} \sum_{k=1}^K L_{\mathcal{D}_k^{\text{te}}}(\phi_k)$ with step size κ .

Considering first a single local SGD update (9) for the context variables, the meta-training update is

finally given as

$$\begin{aligned}\theta \leftarrow \theta - \kappa \nabla_{\theta} \sum_{k=1}^K L_{\mathcal{D}_k^{\text{te}}}(\phi_k) &= (\mathbf{J}_{\theta} \phi_k) \nabla_{\phi_k} L_{\mathcal{D}_k^{\text{te}}}(\phi_k) \\ &= \theta - \kappa \sum_{k=1}^K (I - \eta \nabla_{\theta}^2 L_{\mathcal{D}_k^{\text{r}}}(\theta)) \nabla_{\phi_k} L_{\mathcal{D}_k^{\text{te}}}(\phi_k),\end{aligned}\quad (11)$$

where \mathbf{J}_{θ} represents the Jacobian operation, and $\kappa > 0$ is a step size. With multiple local SGD updating steps (10), we can similarly write the meta-training update as

$$\theta \leftarrow \theta - \kappa \sum_{k=1}^K (I - \eta \nabla_{\theta}^2 L_{\mathcal{D}_k^{\text{r}}}(\theta)) \cdots (I - \eta \nabla_{\phi_k^{m-1}}^2 L_{\mathcal{D}_k^{\text{r}}}(\phi_k^{m-1})) \nabla_{\phi_k^m} L_{\mathcal{D}_k^{\text{te}}}(\phi_k^m). \quad (12)$$

Computation of the Hessian matrices needed in (11) and (12) can be significantly accelerated using a finite difference approximation for Hessian-vector product calculation [29], [30], which is reviewed in Appendix A. The MAML algorithm is summarized in Algorithm 1.

D. FOMAML

First-order MAML (FOMAML) [13] is an approximation of MAML that ignores the second-derivative terms in the meta-training updates (11)–(12). Accordingly, the meta-training update is given as

$$\theta \leftarrow \theta - \kappa \nabla_{\phi_k} \sum_{k=1}^K L_{\mathcal{D}_k^{\text{te}}}(\phi_k). \quad (13)$$

As a result, FOMAML updates parameter θ in the direction of the gradient $\nabla_{\phi_k} \sum_{k=1}^K L_{\mathcal{D}_k^{\text{te}}}(\phi_k)$ instead of $\nabla_{\theta} \sum_{k=1}^K L_{\mathcal{D}_k^{\text{te}}}(\phi_k)$. For some neural network architectures and loss functions, e.g., networks with ReLU activation functions [31], FOMAML has been reported to perform almost as well as MAML [13]. We refer to Algorithm 1 for a summary.

E. REPTILE

REPTILE [14] is a first-order gradient-based meta-learning algorithm as FOMAML. It uses the same local update (9)–(10) for the context variables ϕ_k , but the meta-training update is given as

$$\theta \leftarrow \theta - \kappa \eta \sum_{k=1}^K (\nabla_{\theta} L_{\mathcal{D}_k^{\text{r}}}(\theta) + \nabla_{\phi_k} L_{\mathcal{D}_k^{\text{te}}}(\phi_k)) \quad (14)$$

for the single local gradient update case. Considering (14) with (13) in mind, REPTILE is seen to have the additional term $\nabla_{\theta} L_{\mathcal{D}_k^{\text{r}}}(\theta)$ as compared with FOMAML. When considering $m \geq 1$ local gradient updates for the context variables (eq. (10)), the meta-training update is given as

$$\theta \leftarrow \theta - \kappa \eta \sum_{k=1}^K (\nabla_{\theta} L_{\mathcal{D}_k^{\text{r}}}(\theta) + \nabla_{\phi_k^1} L_{\mathcal{D}_k^{\text{r}}}(\phi_k^1) + \cdots + \nabla_{\phi_k^m} L_{\mathcal{D}_k^{\text{te}}}(\phi_k^m)). \quad (15)$$

For some tasks, REPTILE has been reported to perform in a manner similar to MAML and FOMAML [14]. We refer to [14] for a justification of the method.

Algorithm 1: Few-Pilot Demodulator Meta-Learning via MAML, FOMAML, REPTILE

Input: Meta-training set $\mathcal{D} = \{\mathcal{D}_k\}_{k=1,\dots,K}$ and pilots \mathcal{D}_T from the target device; N^{tr} and N^{te} ; step size hyperparameters η and κ

Output: Learned shared initial parameter vector θ and target-device specific parameter vector ϕ_T

initialize parameter vector θ

meta-learning phase

while not done **do**

for each meta-training device k **do**

 randomly divide \mathcal{D}_k into two sets $\mathcal{D}_k^{\text{tr}}$ of size N^{tr} and $\mathcal{D}_k^{\text{te}}$ of size N^{te}

 compute context variable ϕ_k using (9)–(10)

end

 update shared parameter θ as (11)–(12) (MAML), (13) (FOMAML), (14)–(15) (REPTILE)

end

adaptation on the meta-test device

initialize context parameter vector $\phi_T \leftarrow \theta$

repeat

 draw a pair $(s^{(n)}, y^{(n)})$ from \mathcal{D}_T

 update context variable ϕ_T in the direction of the gradient $\nabla_{\phi_T} \log p(s^{(n)}|y^{(n)}, \phi_T)$ with step size η

until stopping criterion is satisfied

F. CAVIA

Unlike the meta-learning techniques discussed so far, CAVIA [15] interprets context variable ϕ as an additional input to the demodulator, so that the demodulator $p(s|y, \phi, \theta)$ can be written as in (4) with input given by the concatenation $\tilde{y} = [y, \phi]$ and model weights φ equal to the shared parameter vector θ . Using (4), the demodulator is hence in the form $p(s|\tilde{y}, \theta)$, where the shared parameter θ defines the weights of the demodulator model. After meta-training, the shared parameter θ is fixed, and the pilots in set \mathcal{D}_T of the meta-test device are used to optimize the additional input vector ϕ .

In formulas, during meta-training, given the current value of the shared parameter θ , the context variable ϕ_k is optimized by one or more SGD-based update to minimize the loss $L_{\mathcal{D}_k^{\text{tr}}}(\theta)$ as

$$\phi_k \leftarrow \phi_k - \eta \nabla_{\phi_k} L_{\mathcal{D}_k^{\text{tr}}}(\theta). \quad (16)$$

Note that the loss $L_{\mathcal{D}_k^{\text{tr}}}(\theta)$ is a function of ϕ_k through the additional input ϕ_k . With the obtained additional

input ϕ_k , the meta-training update is given as

$$\theta \leftarrow \theta - \kappa \nabla_{\theta} \sum_{k=1}^K L_{\mathcal{D}_k^{\text{te}}}(\theta). \quad (17)$$

After meta-training, as mentioned, parameter θ is fixed, and the context vector ϕ_{T} is obtained by using SGD updates as

$$\phi_{\text{T}} \leftarrow \phi_{\text{T}} - \eta \nabla_{\phi_{\text{T}}} L_{\mathcal{D}_{\text{T}}}(\theta). \quad (18)$$

The CAVIA algorithm is summarized in Algorithm 2.

Algorithm 2: Few-Pilot Demodulator Meta-Learning via CAVIA

Input: Meta-training set $\mathcal{D} = \{\mathcal{D}_k\}_{k=1,\dots,K}$ and pilots \mathcal{D}_{T} from the target device; N^{tr} and N^{te} ; step size hyperparameters η and κ

Output: Learned parameter vector θ and target-device context parameter vector ϕ_{T}

initialize parameter vector θ

meta-learning phase

while not done **do**

for each meta-training device k **do**

initialize context parameter vector ϕ_k

 randomly divide \mathcal{D}_k into two sets $\mathcal{D}_k^{\text{tr}}$ of size N^{tr} and $\mathcal{D}_k^{\text{te}}$ of size N^{te}

 compute context variable ϕ_k using (16)

end

 update shared parameter θ using (17)

end

adaptation on the meta-test device

initialize context parameter vector ϕ_{T}

repeat

 draw a pair $(s^{(n)}, y^{(n)})$ from \mathcal{D}_{T}

 update context parameter vector ϕ_{T} in the direction of the gradient $\nabla_{\phi_{\text{T}}} \log p(s^{(n)} | \tilde{y}^{(n)}, \theta)$ with

 step size η where $\tilde{y}^{(n)} = [y^{(n)}, \phi_{\text{T}}]$

until stopping criterion is satisfied

IV. ONLINE META-LEARNING ALGORITHM

In this section, we consider an online formulation in which packets from devices, containing both pilots and a data payload, are sequentially received at the BS. Therefore, as illustrated in Fig. 3, meta-training

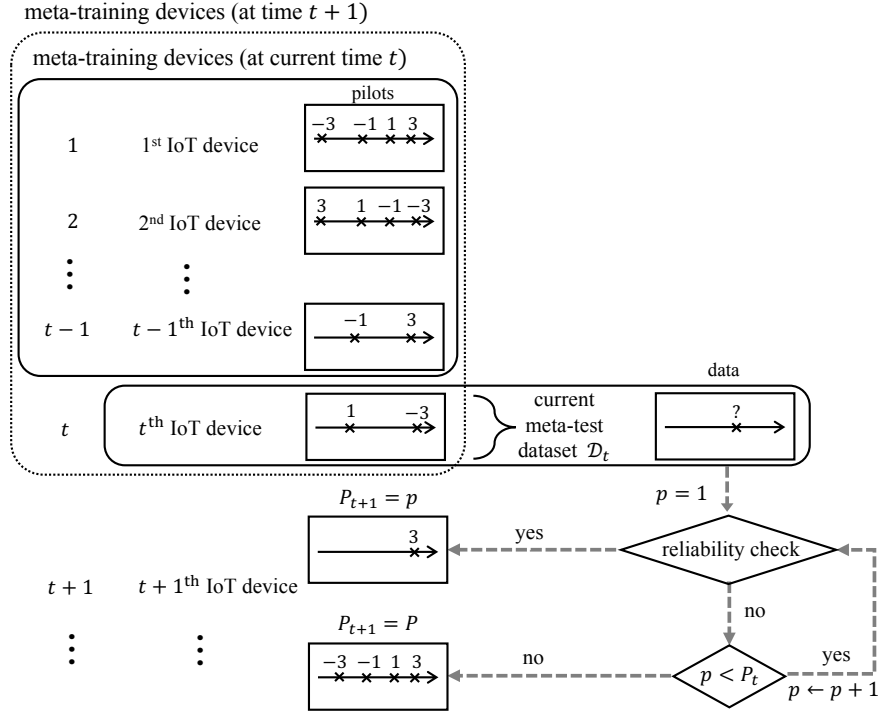


Fig. 5. Illustration of adaptive pilot number selection based on online meta-learning for 4-PAM transmission. The number of transmitted pilots P_{t+1} for the IoT device active in the next time slot is determined by the BS from the performance of the meta-learned demodulator in the current slot t .

data are accumulated at the BS over time. The formulation follows the basic framework of online meta-learning introduced in [16], which proposes an online version of MAML. Here, we adapt the online meta-learning framework to the demodulation problem at hand, and we extend it to integrate all the meta-training solutions discussed in the previous section, namely MAML, FOMAML, REPTILE, and CAVIA. Moreover, we propose a novel adaptive pilot number selection scheme that leverages the fast adaptation property of meta-learning to reduce the pilot overhead.

A. System Model

As illustrated in Fig. 3, in each slot $t = 1, 2, \dots$, the BS receives a packet from a new device, from which the BS obtains the set $\mathcal{D}_t = \{(s_t^{(n)}, y_t^{(n)}) : n = 1, \dots, N_t\}$ of N_t pilots $\{s_t^{(n)}\}$ and corresponding received signals $\{y_t^{(n)}\}$. Each received packet also contains a payload of data $\mathcal{D}_t^{\text{data}} = \{(y_t^{(n)}) : n = 1, 2, \dots\}$. Therefore, at each slot t , the BS has available meta-training data-carrying symbols $\mathcal{D}^{t-1} = \{\mathcal{D}_{t'}\}_{t'=1}^{t-1}$ from previously active devices, as well as meta-test data \mathcal{D}_t from the currently active device. The goal is training a demodulator $p(s|y, \varphi_t)$ that performs well on the payload data $\mathcal{D}_t^{\text{data}}$ after adaptation on the received pilots in set \mathcal{D}_t by making use also of meta-training data \mathcal{D}^{t-1} .

B. Online Learning (Joint Training)

Before discussing online meta-learning, here we briefly summarize the standard online learning set-up as applied to the problem introduced above. As we will discuss, this can be considered as the counterpart of joint training for the offline problem studied in Sec. III-A. In online learning, the goal of the online learner is to determine a model parameter vector φ_t , sequentially at each slot t , that perform well on the loss sequence $L_{\mathcal{D}_t}(\varphi_t)$ for $t = 1, 2, \dots$ (recall (5)). As a benchmark, typical online learning formulations use the best single model φ that can be obtained using knowledge of the losses $L_{\mathcal{D}_t}(\cdot)$ in hindsight for all relevant values of t , i.e., $\varphi \in \arg \min_{\varphi} \sum_t L_{\mathcal{D}_t}(\varphi)$, where the sum is over the time horizon of interest [33].

A standard online learning algorithm is Follow The Leader (FTL) [32], which determines the parameter φ_t that performs best on the previous data \mathcal{D}^{t-1} . For the problem at hand, FTL determines the parameter φ_t at slot t by tackling the problem

$$\varphi_t = \arg \min_{\varphi} \sum_{k=1}^t L_{\mathcal{D}_k}(\varphi). \quad (19)$$

Note that in standard online learning formulations the sum in (19) would be performed up to time $t - 1$ due to the typical assumption that no data is a priori known at time t about loss $L_{\mathcal{D}_t}(\cdot)$ [33]. From (19), FTL can be interpreted as a form of joint training carried out in an online manner. From a theoretical standpoint, FTL can be shown to obtain a sub-linearly growing regret with respect to slot t as compared to the discussed benchmark learner with hindsight information (see [33] for precise statements).

C. Online Meta-Learning

With meta-learning, as discussed in Sec. III-B (see Fig. 4), the demodulator $p(s|y, \phi, \theta)$ is defined by a shared parameter θ and by a context, device-dependent, variables ϕ . In the online setting at hand, in each slot t , we propose to estimate the shared parameter θ_t from the meta-training data \mathcal{D}^{t-1} , while the context variable ϕ_t for the currently active device is estimated from \mathcal{D}_t . These steps can be carried out for different meta-learning strategies as described in Sec. III, with set \mathcal{D}^{t-1} in lieu of the meta-training set \mathcal{D} and set \mathcal{D}_t for the meta-test set \mathcal{D}_T . As a special case, if MAML is used, this recovers the Follow The Meta Leader (FTML) algorithm [16], which determines the shared parameter θ_t by solving the problem

$$\theta_t = \arg \min_{\theta} \sum_{k=1}^{t-1} L_{\mathcal{D}_k^{\text{te}}}(\phi_t), \quad (20)$$

where the context variable ϕ_t is computed from the local updates (9)–(10) starting from the initial value θ . The general algorithm for online meta-learning is summarized in Algorithm 3.

Algorithm 3: Few-Pilot Demodulator Online Meta-Learning

Input: Data sets $\{\mathcal{D}_t, \mathcal{D}_t^{\text{data}}\}$ for $t = 1, 2, \dots$; step size hyperparameters η and κ ; number of transmitted pilots p

Output: Learned parameter vector θ_t and context vector ϕ_t , for $t = 1, 2, \dots$

initialize parameter vector θ_1

initialize the meta-training dataset \mathcal{D} as empty, i.e., $\mathcal{D} \leftarrow []$

for $t = 1, \dots$ **do**

 receive $\mathcal{D}_t = \{(s_t^{(n)}, y_t^{(n)}) : n = 1, \dots, p\}$

 adaptation on the current device

 setting $\mathcal{D}_T \leftarrow \mathcal{D}_t$

 follow *adaptation on the meta-test device* in Algorithm 1 or Algorithm 2 to obtain context vector

$\phi_T \rightarrow \phi_t$

 use ϕ_t, θ_t to demodulate $\mathcal{D}_t^{\text{data}}$

 meta-learning phase

 add current dataset \mathcal{D}_t to meta-training dataset \mathcal{D} as $\mathcal{D} \leftarrow \bigcup_{k=1}^t \mathcal{D}_k$

 follow *meta-learning phase* in Algorithm 1 or Algorithm 2 to obtain shared parameter θ_{t+1}

end

D. Integrated Online Meta-Learning and Pilot Allocation

In order to further reduce the pilot overhead, we now consider the possibility to adapt the number of transmitted pilot symbols in each slot t based on the performance of the demodulator meta-learned in the previous slots. We note that in [34] the idea of adapting the number of pilots was proposed for a single device by leveraging the temporal correlation of the channels for an individual device. In contrast, the method proposed here works by using information from different devices without making any assumption about temporal correlations.

In the proposed scheme, at each slot t , a device transmits P_t pilots. The BS carries out demodulation of the data payload by using the demodulator $p(s|y, \phi_t^{(p)}, \theta_t)$, where the shared parameter θ_t is obtained as discussed in Sec. IV-C and the context variable $\phi_t^{(p)}$ is obtained by using $p \leq P_t$ pilots via Algorithm 3. By trying different values of $p = 1, \dots, P_t$, the BS determines the minimum value of $p \leq P_t$ such that demodulation of the data in set $\mathcal{D}_t^{\text{data}}$ meets some reliability requirement. If such a value of p is found, then the BS assigns the number of pilots for the next slot as $P_{t+1} = p$. Otherwise, we set P_{t+1} to the maximum value P . The overall online meta-learning procedure with pilot allocation scheme is summarized in Algorithm 4, and an illustration of the proposed adaptive pilot number selection strategy can be found

Algorithm 4: Few-Pilot Demodulator Learning via Online Meta-Learning with Adaptive Pilot Number Selection

Input: Data sets $\{\mathcal{D}_t, \mathcal{D}_t^{\text{data}}\}$ for $t = 1, 2, \dots$; step size hyperparameters η and κ

Output: Learned parameter vector θ_t and context vector ϕ_t , for $t = 1, 2, \dots$

initialize parameter vector θ_1

initialize the meta-training dataset \mathcal{D} as empty, i.e., $\mathcal{D} \leftarrow []$

initialize number of transmitted pilots $P_1 \leftarrow P$

for $t = 1, \dots$ **do**

receive $\mathcal{D}_t = \{(s_t^{(n)}, y_t^{(n)}) : n = 1, \dots, P_t\}$

adaptation on the current device

for $p = 1, \dots, P_t$ **do**

setting $\mathcal{D}_T \leftarrow \{(s_t^{(n)}, y_t^{(n)}) : n = 1, \dots, p\}$

follow *adaptation on the meta-test device* in Algorithm 1 or Algorithm 2 to obtain context vector $\phi_T \rightarrow \phi_t$

if (*reliability check passed*) **then**

set $P_{t+1} = p$ and exit

else if (*reliability check not passed*) and ($p = P_t$) **then**

set $P_{t+1} = P$

end

use ϕ_t, θ_t to demodulate $\mathcal{D}_t^{\text{data}}$

meta-learning phase

add current dataset \mathcal{D}_t to meta-training dataset \mathcal{D} as $\mathcal{D} \leftarrow \bigcup_{k=1}^t \mathcal{D}_k$

follow *meta-learning phase* in Algorithm 1 or Algorithm 2 to obtain shared parameter θ_{t+1}

end

in Fig. 5.

In practice, the reliability level can be estimated in different ways. For example, it can be obtained by evaluating the output of a cyclic redundancy check (CRC) field at the output of a decoder operating on the demodulated symbols from the payload $\mathcal{D}_t^{\text{data}}$. Here, we consider a simpler approach that uses directly the output of the demodulator $p(s|y, \phi_t, \theta_t)$ without having to run a decoder. This is done by comparing the cross-entropy loss (5) on the demodulated data

$$- \sum_{y \in \mathcal{D}_t^{\text{data}}} \max_s [\log p(s|y, \phi_t^{(p)}, \theta_t)] \quad (21)$$

to some prescribed threshold: if (21) is below a threshold, then the reliability check is considered successful.

V. EXPERIMENTS

In this section, we provide numerical results in order to bring insights into the advantages of meta-learning. Code is available at <https://github.com/sangwoo-p/meta-demodulator>.

A. Offline Meta-Learning: Binary Fading

We begin by considering the offline set-up and focusing on a simple example, in which we assume an ideal transmitter, i.e., $x_k = s_k$ and fading is binary, i.e., the channel h_k in (1) can take values ± 1 . This simplified model will be useful to build some intuition about the operation of meta-learning. We adopt pulse-amplitude modulation with four amplitude levels (4-PAM) $\mathcal{S} = \{-3, -1, 1, 3\}$. Pilot symbols in the meta-training dataset \mathcal{D} and meta-test dataset \mathcal{D}_T follow a fixed periodic sequence $-3, -1, 1, 3, -3, -1, \dots$, while transmitted symbols in the test set for the meta-test device are randomly selected from the set \mathcal{S} . The channel of the meta-test device is selected randomly between $+1$ and -1 with equal probability, while the channels for half of the meta-training devices are set as $+1$ and for the remaining half as -1 .

Other numerical details are as follows. The number of meta-training devices is $K = 20$; the number of pilot symbols per device is $N = 8$, which we divide into $N^{\text{tr}} = 4$ meta-training samples and $N^{\text{te}} = 4$ meta-testing samples. The demodulator (4) is a neural network with $L = 3$ layers, i.e., an input layer with 2 neurons, one hidden layer with 30 neurons, and a softmax output layer with 4 neurons. The network adopts a hyperbolic tangent function $\sigma(\cdot) = \tanh(\cdot)$ as the activation function. For meta-learning, we use a minibatch of size 4 with fixed learning rates $\eta = 0.1$ and $\kappa = 0.025$. The weights and biases are all initialized to 1. For the training in meta-test device, we adopt a minibatch of size 1 and learning rate $\eta = 0.1$. The signal-to-noise ratio (SNR) is given as $\mathbb{E}[s_k^2]/N_0 = 15\text{dB}$.

We compare the performance of the proposed meta-learning approach via MAML, FOMAML, REPTILE, and CAVIA with: (i) a fixed initialization scheme where data from the meta-training devices is not used; (ii) joint training with the meta-training dataset \mathcal{D} as explained in Sec. III-A; (iii) optimal ideal demodulator that assumes perfect channel state information. For (ii), we set the learning rate to 0.01 and the minibatch size to 4. The probability of error of (iii) can be computed as $P_e = 3/2Q(\sqrt{\text{SNR}/5})$ using standard arguments.

In Fig. 6, we plot the average probability of symbol error with respect to number P of pilots for the meta-test device. All of the meta-learning approaches are seen to vastly outperform the mentioned baseline approaches by adapting to the channel of the meta-test device using only a few pilots. In contrast, joint training fails to perform better than fixed initialization. For a very small number P of pilots, CAVIA is

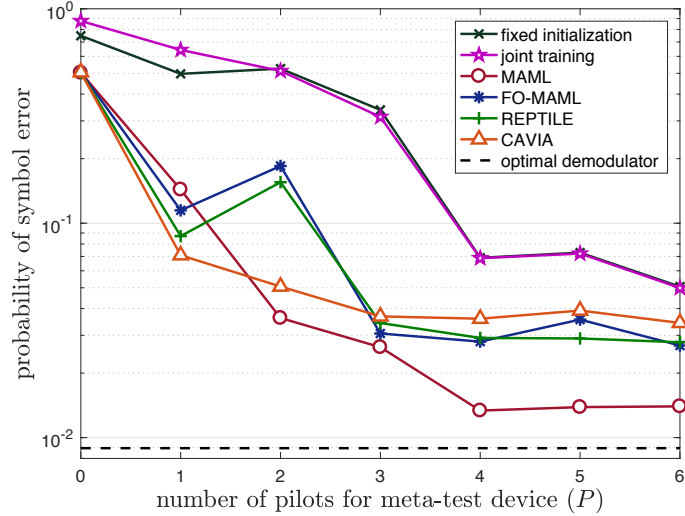


Fig. 6. Probability of symbol error with respect to number P of pilots for the meta-test device for an offline meta-learning example with binary fading and no amplifier distortion. MAML, fixed initialization, joint training starts from same fixed initialization point of all the weights set to 1. REPTILE, FOMAML, CAVIA starts from a random initialization point. We use step sizes $\eta = 0.1$ and $\kappa = 0.025$ for all schemes. Probability of symbol error is averaged over 1000 data symbols and 100 meta-test devices.

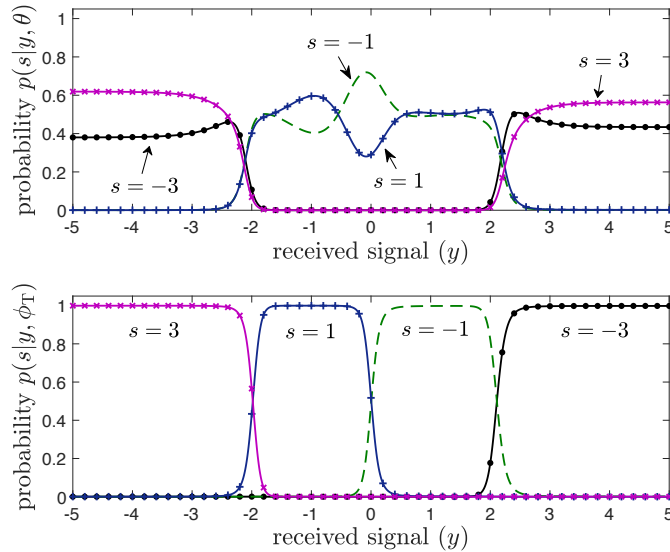


Fig. 7. (Top) Demodulator (4) for the shared parameter vector θ obtained via offline meta-learning phase in Algorithm 1 using MAML; (Bottom) Updated demodulator with target-device specific parameter vector ϕ_T (4) using $P = 4$ pilots from the meta-test device.

seen to be the best solution, while MAML outperforms all other schemes for larger values of P . This accounts for the different inductive biases captured by the two methods. MAML has more flexibility in choosing the shared parameter θ thanks to the application of local updates that yield the demodulator weight vector ϕ_T . This is unlike CAVIA in which the demodulator weight vector is fixed to the shared parameter θ . The flexibility of MAML has the potential of improving the meta-test performance, but this comes at the cost of requiring a larger number of pilots. Overall, these results confirm the claim

that, unlike conventional solutions, meta-training can effectively transfer information from meta-training devices to a new target device.

In order to gain intuition on how meta-learning learns from the meta-training devices, in Fig. 7, we plot the probabilities defined by the demodulator (4) for the four symbols in the constellation \mathcal{S} with the shared parameter vector θ obtained from the meta-learning phase in Algorithm 1 (top) and with target-device specific parameter vector ϕ_T after adaptation using the pilots of the target meta-test device (bottom). We adopted MAML as the meta-learning algorithm. The class probabilities identified by meta-learning in the top figure have the interesting property of being approximately symmetric with respect to the origin. This makes the resulting decision region easily adaptable to the channel of the target device, which may take values ± 1 in this example. The adapted probabilities in the bottom figure illustrate how the initial demodulator obtained via MAML is specialized to the channel of the target device.

B. Offline Meta-Learning: Rayleigh Fading and Transmitters' Distortion

We now consider a more realistic scenario including Rayleigh fading channels $h_k \sim \mathcal{CN}(0, 1)$ and model (3) to account for amplifier's distortions at the transmitters, where $\alpha_k = 4$ and β_k is uniformly distributed in the interval $[0.05, 0.15]$. We assume 16-ary quadrature amplitude modulation (16-QAM) for constellation \mathcal{S} and the sequence of pilot symbols in the meta-training dataset \mathcal{D} and meta-test dataset \mathcal{D}_T was fixed by cycling through the symbols in \mathcal{S} (the sequence used in the experiment is detailed in Appendix B), while the transmitted symbols in the test set for the meta-test device are randomly selected from \mathcal{S} . The number of meta-training devices is set as $K = 100$; the number of pilot symbols per device is $N = 32$, which we divide into $N^{\text{tr}} = 16$ meta-training samples and $N^{\text{te}} = 16$ meta-testing samples. The SNR is given as $\mathbb{E}[s_k^2]/N_0 = 15\text{dB}$. Further details on the numerical set-up can be found in Appendix B.

In Fig. 8, we plot the average probability of symbol error with respect to number of local updates m . Note that the average is taken over noise as well as over the fading channels. As can be seen from Fig. 8, the best number of local updates m depends on meta-training technique: $m = 7$ is preferable for MAML, $m = 8$ for FOMAML, $m = 9$ for REPTILE, and $m = 2$ for CAVIA. We use these settings for all of the upcoming experiments. Except for CAVIA, single local updates, i.e., $m = 1$, do not lead to effective meta-learning in this example. Assuming more local updates hence allows meta-learning algorithms not to impose too stringent conditions on the shared parameter θ used by MAML, FOMAML, and REPTILE as the initial point for local updates. In contrast, under CAVIA, local adaptation takes place via the additional input vector ϕ , which is less demanding in terms of number of updates. MAML and CAVIA are seen to offer the best performance when m is properly optimized.

In Fig. 9, we plot the average probability of symbol error with respect to number P of pilots for the meta-test device. As in Fig. 6, we compare the performance of meta-training methods with fixed

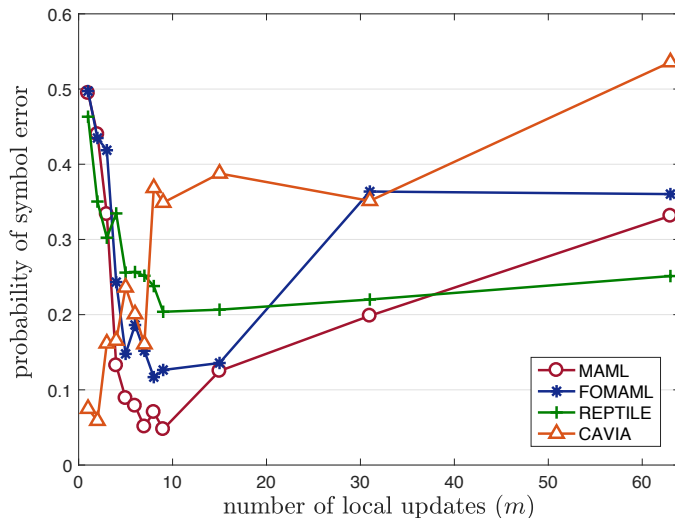


Fig. 8. Probability of symbol error with respect to number m of local updates for offline meta-training for 16-QAM scenario with Rayleigh fading and amplifier distortion for $K = 100$ meta-training devices, $N^{\text{tr}} + N^{\text{te}} = 32$ pilots for meta-training devices, and $P = 8$ pilots for meta-test devices. Probability of symbol error is averaged over by 1000 data symbols and 100 meta-test devices.

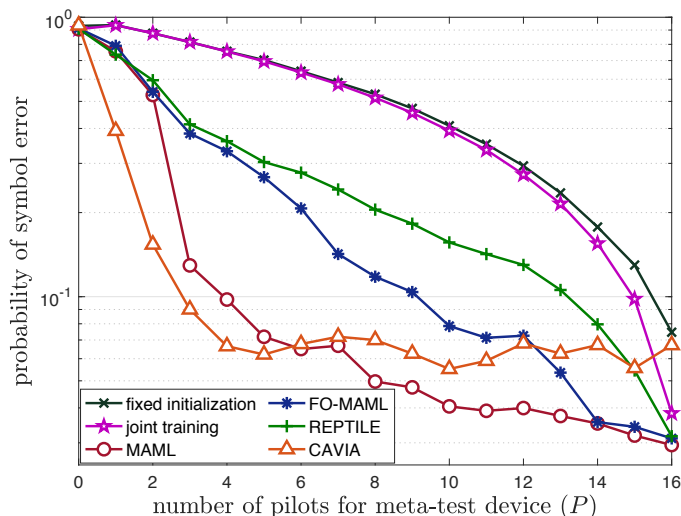


Fig. 9. Probability of symbol error with respect to number P of pilots for the meta-test devices for an offline meta-learning example with 16-QAM, Rayleigh fading, and amplifier distortion for $K = 100$ meta-training devices, $N^{\text{tr}} + N^{\text{te}} = 32$ pilots for meta-training devices, $m = 7, 8, 9, 2$ for local updates of MAML, FOMAML, REPTILE, and CAVIA, respectively. Probability of symbol error is averaged over by 1000 data symbols and 100 meta-test devices.

initialization and joint training strategies. All of the meta-training approaches are seen to adapt more quickly than the baseline schemes to the channel and non-linearity of the target device. Confirming the results in Fig. 6, MAML shows the best performance for sufficiently large P , while CAVIA shows the fastest adaptation by requiring fewer pilots as compared to other techniques. Joint training shows similar performance as compared to fixed initialization, which may be attributed to a failure of joint training to transfer useful information from meta-training devices.

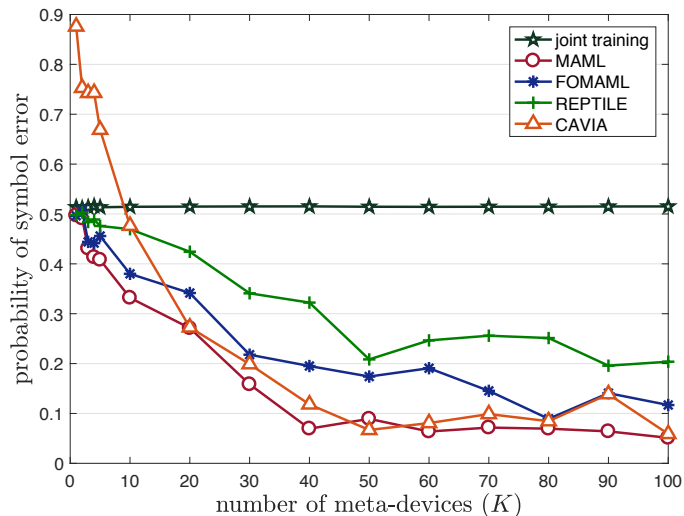


Fig. 10. Probability of symbol error with respect to number K of meta-training device for 16-QAM scenario with Rayleigh fading and amplifier distortion with $N^r + N^{te} = 32$ pilots for meta-training devices, $P = 8$ pilots for meta-test devices, and $m = 7, 8, 9, 2$ for local updates of MAML, FOMAML, REPTILE, and CAVIA, respectively. Probability of symbol error is averaged over by 1000 data symbols and 100 meta-test devices.

Finally, in Fig. 10, we plot the average probability of symbol error with respect to the number K of meta-training devices. Following the discussion above, joint training cannot benefit from an increasing value of K . In contrast, all of the meta-training techniques show better performance when given more meta-training devices, up to a point where the gain saturates. This matches well with the intuition that there is only a limited amount of common information among different users that can be captured by meta-learning. Confirming the results in Fig. 8 and Fig. 9, MAML and CAVIA are seen to offer best performance when given sufficient number K of meta-training devices. Furthermore, CAVIA needs a larger value of K than MAML. This accounts again for CAVIA’s architectural difference as compared to MAML: CAVIA needs to find a shared parameter vector θ for the demodulator $p(s|y, \phi_T, \theta)$ that is not adapted to the training symbols of the current device.

C. Online Meta-Learning

We now move on to consider the online scenario under same assumptions on Rayleigh fading, transmitters’ distortion, modulation scheme, and SNR as in the offline set-up presented in Sec. V-B.

The maximum number of pilots is set as $P = 32$, and we used adaptive pilot number selection scheme in Algorithm 4 to determine the number of pilots P_t in any slot t . In a manner similar to the offline set-up, we compare the performance with: (i) a fixed initialization scheme that only adapts to current device based on current pilot data \mathcal{D}_t with number of pilots P_t fixed as constant to a prescribed value; (ii) joint training as described in Sec. IV-B. Other details on the numerical set-up can be found in Appendix B.

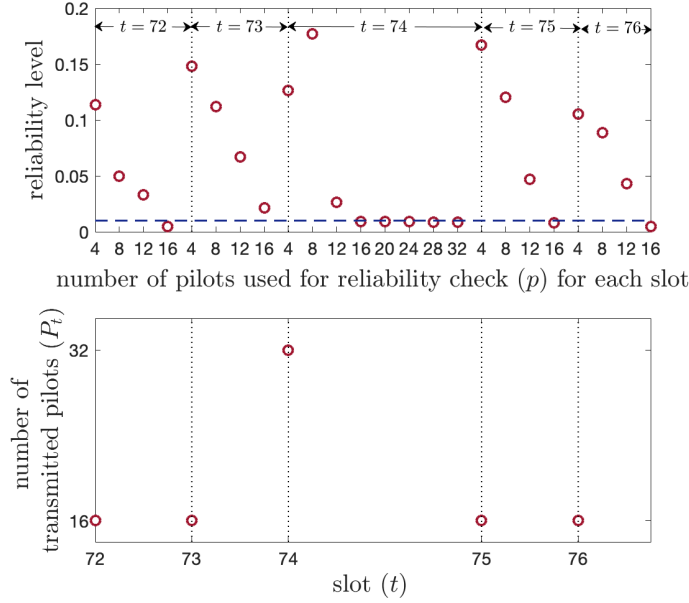


Fig. 11. Illustration of the procedure of adaptive pilot number selection scheme: (top) reliability level in (21) versus the number p of pilots during slots $t = 72, \dots, 76$ (the prescribed reliability threshold value, 0.01, is dashed); (bottom) number of transmitted pilots P_t for each slot $t = 72, \dots, 76$.

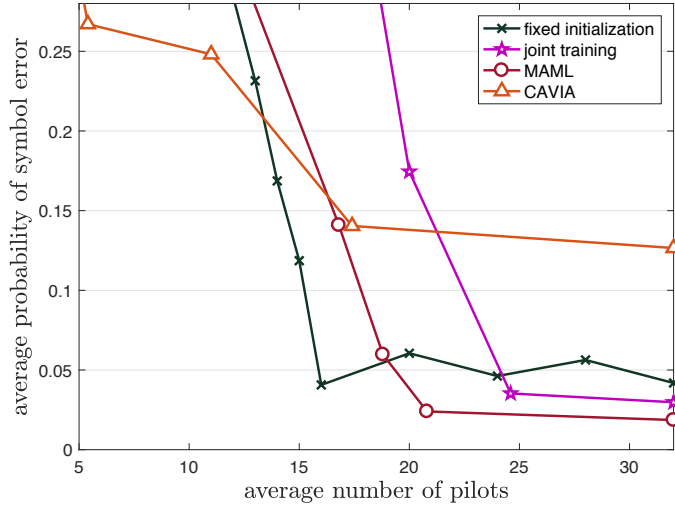


Fig. 12. Average probability of symbol error with respect to average number of pilots over slots $t = 71, \dots, 90$ for online meta-learning.

In Fig. 11, we first describe the procedure used by the proposed adaptive pilot number selection scheme. As discussed in Sec. IV-D, we evaluate reliability levels for different values of the number p of pilots using (21) as shown in Fig. 11 (top) and the number of transmitted pilots P_{t+1} in the next slot is selected accordingly (bottom). The adaptive pilot number selection scheme is performed here with MAML, while the prescribed threshold value is set as 0.01. For instance, for slot 73, the number of transmitted pilots is chosen as $P_{73} = 16$ based on the result from previous slot 72 that passed reliability check at $p = 16$. In contrast, for slot 74, the number of transmitted pilots $P_{74} = P$ has been chosen as maximum value

$p = 32$ due to the failure of reliability check pass at slot 73. In the following, we assess whether the adaptive pilot number selection scheme can maintain reasonable performance in terms of probability of symbol error in the payload data $\mathcal{D}_t^{\text{data}}$, despite the illustrated reduction in the pilot overhead.

To this end, in Fig. 12, we plot the average probability of symbol error for payload data $\mathcal{D}_t^{\text{data}}$ versus the average number of transmitted pilots as evaluated in the period $t = 71, \dots, 90$. For joint training, MAML, and CAVIA, the corresponding curve is obtained by selecting the threshold values $(0.00001, 0.01, 0.1)$, $(0.00001, 0.01, 0.03, 0.05)$, and $(0.00001, 0.2, 0.4, 0.5)$, respectively, for the reliability level. For fixed initialization, each point on the curve corresponds to the given fixed number of pilots defined by the horizontal axis. The proposed adaptive pilot number selection scheme is seen to improve over fixed initialization. In particular, in a manner consistent with the discussion so far, MAML can operate with as few as 20 pilots on average while outperforming fixed initialization and joint training using 32 pilots. For lower average values of the number of pilots, CAVIA shows the best performance.

VI. CONCLUSIONS AND EXTENSIONS

In communication systems with short packets, such as IoT, meta-learning techniques can adapt quickly based on few training examples by transferring knowledge from previously observed pilot information from other devices. In this paper, we have proposed the use of offline and online meta-learning for IoT scenarios by adapting state-of-the-art meta-learning schemes, namely MAML, FOMAML, REPTILE, and CAVIA, in a unified framework. For the online setting, we have further integrated meta-learning with an adaptive pilot number selection scheme to reduce the pilot overhead. Extensive numerical results have validated the advantage of meta-learning in both offline and online cases as compared to conventional machine learning schemes. Moreover, comparisons among the mentioned meta-learning schemes reveal that MAML and CAVIA are preferable, with each scheme outperforming the other in different regimes in terms of amount of available meta-training data. For online meta-learning, we have showed the feasibility of the proposed pilot selection scheme by demonstrating a decreased pilot overhead with negligible performance degradation of the demodulator.

Meta-learning, first introduced in the conference version [2] of this work and in [17] for use in communications systems, may be useful in a number for other network functionalities characterized by reduced overhead and correlation across successive tasks. Examples include prediction of traffic from sets of IoT devices, e.g., in grant-free access [36], [37]; channel estimation [18]; and precoding in multi-antenna systems. Furthermore, more advanced meta-training solutions can also be considered that are based on a probabilistic estimate of the context variables [27]. Finally, this work may motivate the development of novel meta-training techniques that reap the complementary benefits of CAVIA and MAML.

APPENDIX A

HESSIAN-VECTOR PRODUCT CALCULATION

In order to compute the updates in (11) and (12), we adopt a finite difference method for Hessian-vector product calculation [29]. This allows us to avoid computing Hessian matrix, obtaining an approximate value of the product of the Hessian matrix and a vector. Given a loss function $L(\theta)$ defined and doubly continuously differentiable over a local neighborhood of the value θ of interest, the finite difference method approximates the Hessian-vector product Hg , where $H = \nabla_{\theta}^2 L(\theta)$ is the Hessian matrix and g is any vector. The Hessian-vector product Hg can be approximately computed as [29]

$$Hg \approx \frac{1}{\alpha}(\nabla_{\theta} L(\theta + \alpha g) - \nabla_{\theta} L(\theta)), \quad (22)$$

where α is a sufficiently small constant value. In (22), we follow [30] to choose α as

$$\alpha = \frac{2\sqrt{\epsilon}(1 + \|\theta\|)}{\|g\|}, \quad (23)$$

where $\|\cdot\|$ indicates Euclidean norm and $\epsilon = 1.1920929e-7$, which is an upper bound on the relative error due to rounding in single precision floating-point arithmetic [35].

APPENDIX B

DETAILS ON NUMERICAL SET-UP

A. Offline Meta-Learning

The following is the fixed sequence that is used for pilot symbols in the meta-training dataset \mathcal{D} and meta-test dataset \mathcal{D}_T in the offline scenario: $1 + 1j, 1 - 3j, -3 + 1j, 3 + 3j, 3 + 1j, -1 - 1j, -1 - 3j, -3 - 3j, 3 - 1j, -1 + 3j, -1 + 1j, 1 - 1j, -3 - 1j, 1 + 3j, -3 + 3j, 3 - 3j, 1 + 1j, 1 - 3j, \dots$. For the experiments in Sec. V-B, every demodulators (4) except for CAVIA is a neural network with $L = 5$ layers, i.e., an input layer with 2 neurons, three hidden layer with 10, 30, 30 neurons each, and a softmax output layer with 16 neurons. For CAVIA, we use a neural network with an input layer of 12 neurons, three hidden layer with 10, 30, 30 neurons each, and a softmax output layer with 16 neurons, so that the dimension of the context parameter ϕ is 10. For the activation function, we adopt a rectified linear unit $\sigma(\cdot) = \text{ReLU}(\cdot)$. For the training with meta-training data \mathcal{D} , we use a minibatch of size 4 with learning rates $\eta = 0.001$ and $\kappa = 0.001$ for MAML and FOMAML; learning rates $\eta = 0.01$ and $\kappa = 0.01$ for REPTILE; learning rates $\eta = 1$ and $\kappa = 0.001$ for CAVIA; and learning rate $\eta = 0.001$ for joint training. We randomly sampled 4 pilots among whole 32 pilots to compose one minibatch. The weights and biases are initialized randomly. For the training in meta-test device, we adopt a minibatch of size 1 and learning rate $\eta = 0.001$ for MAML, FOMAML, REPTILE, and joint training; and learning rate $\eta = 1$ for CAVIA.

B. Online Meta-Learning

For the experiments in Sec. V-C, the pilot sequences in \mathcal{D}_t are chosen based on rejection sampling method so that, for any successive four pilots, there exists one pilot with minimum magnitude, two pilots with median magnitude, and one pilot with maximum magnitude, while also guaranteeing that any successive sixteen pilots for the same device include all constellation symbols set \mathcal{S} . We trained the demodulator (4) with same minibatch sizes and learning rates described above for offline meta-learning and we sampled 4 pilots without replacement to compose one minibatch. The number of local updates m is chosen using the values used for Fig. 9 and Fig. 10.

REFERENCES

- [1] J. Östman, G. Durisi, E. G. Ström, M. C. Coşkun, and G. Liva, “Short packets over block-memoryless fading channels: Pilot-assisted or noncoherent transmission?” *IEEE Trans. Commun.*, vol. 67, no. 2, pp. 1521–1536, Feb. 2019.
- [2] S. Park, H. Jang, O. Simeone, and J. Kang, “Learning how to demodulate from few pilots via meta-learning,” in *Proc. IEEE Signal Processing Advances in Wireless Commun. (SPAWC)*, Cannes, France, July 2019.
- [3] M. Ibnkahla, “Applications of neural networks to digital communications—a survey,” *Signal processing*, vol. 80, no. 7, pp. 1185–1215, July 2000.
- [4] O. Simeone, “A very brief introduction to machine learning with applications to communication systems,” *IEEE Trans. Cognitive Commun. and Netw.*, vol. 4, no. 4, pp. 648–664, Nov. 2018.
- [5] S. Bouchired, D. Roviras, and F. Castanié, “Equalisation of satellite mobile channels with neural network techniques,” *Space Communications*, vol. 15, no. 4, pp. 209–220, 1998/1999.
- [6] T. O’Shea and J. Hoydis, “An introduction to deep learning for the physical layer,” *IEEE Trans. Cognitive Commun. and Netw.*, vol. 3, no. 4, pp. 563–575, Dec. 2017.
- [7] S. Dörner, S. Cammerer, J. Hoydis, and S. ten Brink, “Deep learning based communication over the air,” *IEEE Journal of Selected Topics in Signal Processing*, vol. 12, no. 1, pp. 132–143, 2017.
- [8] M. Khani, M. Alizadeh, J. Hoydis, and P. Fleming, “Adaptive neural signal detection for massive mimo,” *arXiv preprint arXiv:1906.04610*, 2019.
- [9] A. G. Helmy, M. Di Renzo, and N. Al-Dhahir, “On the robustness of spatial modulation to I/Q imbalance,” *IEEE Commun. Letters*, vol. 21, no. 7, pp. 1485–1488, July 2017.
- [10] S. Thrun, “Lifelong learning algorithms,” in *Learning to learn*. Springer, 1998, pp. 181–209.
- [11] E. Grant, C. Finn, S. Levine, T. Darrell, and T. Griffiths, “Recasting gradient-based meta-learning as hierarchical bayes,” *arXiv preprint arXiv:1801.08930*, 2018.
- [12] O. Vinyals, C. Blundell, T. Lillicrap, K. Kavukcuoglu, and D. Wierstra, “Matching networks for one shot learning,” in *Proc. Advances in Neural Information Processing Systems (NIPS)*, 2016, pp. 3630–3638.
- [13] C. Finn, P. Abbeel, and S. Levine, “Model-agnostic meta-learning for fast adaptation of deep networks,” *arXiv preprint arXiv:1703.03400*, 2017.
- [14] A. Nichol, J. Achiam, and J. Schulman, “On first-order meta-learning algorithms,” *arXiv preprint arXiv:1803.02999*, 2018.
- [15] L. Zintgraf, K. Shiarli, V. Kurin, K. Hofmann, and S. Whiteson, “Fast context adaptation via meta-learning,” in *Proc. International Conference on Machine Learning (ICML)*, 2019, pp. 7693–7702.
- [16] C. Finn, A. Rajeswaran, S. Kakade, and S. Levine, “Online meta-learning,” *arXiv preprint arXiv:1902.08438*, 2019.
- [17] Y. Jiang, H. Kim, H. Asnani, and S. Kannan, “Mind: Model independent neural decoder,” in *Proc. IEEE Signal Processing Advances in Wireless Commun. (SPAWC)*, Cannes, France, July 2019.
- [18] H. Mao, H. Lu, Y. Lu, and D. Zhu, “RoemNet: Robust meta learning based channel estimation in OFDM systems,” in *Proc IEEE Int. Conf. Commun. (ICC)*, Shanghai, China, May 2019.
- [19] E. Costa and S. Pupolin, “M-QAM-OFDM system performance in the presence of a nonlinear amplifier and phase noise,” *IEEE Trans. Commun.*, vol. 50, no. 3, pp. 462–472, Mar. 2002.
- [20] M. Windisch and G. Fettweis, “On the performance of standard-independent I/Q imbalance compensation in OFDM direct-conversion receivers,” in *Proc. IEEE European Signal Processing Conference*, pp. 1–5, Antalya, Turkey, Sep. 2005.
- [21] C. M. Bishop, *Pattern recognition and machine learning*. Springer, 2006.
- [22] O. Simeone, “A brief introduction to machine learning for engineers,” *Foundations and Trends® in Signal Processing*, vol. 12, no. 3-4, pp. 200–431, 2018.
- [23] I. Goodfellow, Y. Bengio, and A. Courville, *Deep Learning*. MIT Press, 2016.
- [24] D. Koller and N. Friedman, *Probabilistic graphical models: principles and techniques*. MIT Press, 2009.

- [25] S. Ravi and A. Beatson, “Amortized bayesian meta- learning,” in *Proc. International Conference on Learning Representations (ICLR)*, 2019.
- [26] J. Gordon, J. Bronskill, M. Bauer, S. Nowozin, and R. Turner, “Meta-learning probabilistic inference for prediction,” in *Proc. International Conference on Learning Representations (ICLR)*, 2019.
- [27] C. Nguyen, T.-T. Do, and G. Carneiro, “Uncertainty in model-agnostic meta-learning using variational inference,” *arXiv preprint arXiv:1907.11864*, 2019.
- [28] A. Antoniou, H. Edwards, and A. Storkey, “How to train your MAML,” *arXiv preprint arXiv:1810.09502*, 2018.
- [29] Y. A. LeCun, L. Bottou, G. B. Orr, and K.-R. Müller, “Efficient backprop,” in *Neural networks: Tricks of the trade*. pp. 9–48, Springer, 2012.
- [30] N. Andrei, “Accelerated conjugate gradient algorithm with finite difference Hessian/vector product approximation for unconstrained optimization,” *Journal of Computational and Applied Mathematics*, vol. 230, no. 2, pp. 570–582, Aug. 2009.
- [31] I. J. Goodfellow, J. Shlens, and C. Szegedy, “Explaining and harnessing adversarial examples,” *arXiv preprint arXiv:1412.6572*, 2014.
- [32] J. Hannan, “Approximation to bayes risk in repeated play,” *Contributions to the Theory of Games*, vol. 3, pp. 97–139, 1957.
- [33] S. Shalev-Shwartz, “Online learning and online convex optimization,” *Foundations and Trends® in Machine Learning*, vol. 4, no. 2, pp. 107–194, 2012.
- [34] O. Simeone and U. Spagnolini, “Adaptive pilot pattern for OFDM systems,” in *Proc IEEE Int. Conf. Commun. (ICC)*, pp. 978–982, Paris, France, June 2004.
- [35] D. Goldberg, “What every computer scientist should know about floating-point arithmetic,” *ACM Computing Surveys (CSUR)*, vol. 23, no. 1, pp. 5–48, 1991.
- [36] R. Kassab, O. Simeone, and P. Popovski, “Information-centric grant-free access for IoT fog networks: Edge vs cloud detection and learning,” *arXiv preprint arXiv:1907.05182*, 2019.
- [37] N. Jiang, Y. Deng, O. Simeone, and A. Nallanathan, “Online supervised learning for traffic load prediction in framed-ALOHA networks,” *IEEE Commun. Letters*, 2019.
- [38] J. Ahn, O. Simeone, and J. Kang, “Wireless federated distillation for distributed edge learning with heterogeneous data,” *arXiv preprint arXiv:1907.02745*, 2019.